Two-photon Rabi splitting and optical Stark effect in semiconductor microcavities

I. Carusotto
Scuola Normale Superiore and INFM, Piazza dei Cavalieri 7, 56126 Pisa, Italy

G. C. La Rocca
Dipartimento di Fisica, Università di Salerno, 84081 Baronissi (Sa), Italy
and INFM, Scuola Normale Superiore, Piazza dei Cavalieri 7, 56126 Pisa, Italy
(Received 11 January 1999)

We have studied two-photon nonlinear optical effects arising in a microcavity geometry from resonant two-photon absorption or second-harmonic generation. The transmission spectrum of the cavity is shown to depend on light intensity according to a simple two-level picture with an intensity-dependent coupling: at resonance the system exhibits a two-photon Rabi splitting. The absorption spectrum of a weak probe beam in a pumped cavity is found to strongly depend on pump intensity and detuning; the resulting effect is a sort of two-photon analogue of the usual optical Stark effect. For moderate pump intensities a two-level picture with a pump-dependent coupling can account for the main results, while at higher intensities new unexpected features show up; in particular, we predict the appearance of gain in well-determined spectral regions due to hyper-Raman processes. Finally, we have shown how the coupling coefficients appearing in our formalism can be obtained from a detailed knowledge of the material and geometrical properties of a specific system. For illustrative purposes, we have estimated the required light intensities using realistic data for a GaAs-based semiconductor microcavity. [S0163-1829(99)00932-7]

I. INTRODUCTION

The recent progress of semiconductor technology has made possible the actual realization of solid-state optical devices that allow for the observation of both quantum and nonlinear optical effects. The investigation of fundamental effects in light-matter interaction has had an enormous development thanks to the use of laser sources, which provide light fields of remarkable monochromaticity and intensity. Most experiments were carried out on gaseous samples, in order to have optical transitions with a linewidth very close to the natural radiative one.[1,2] In this way it is possible to perform the experiments of interest without being disturbed by collisional and disorder-induced damping effects. Very recently, laser cooling and trapping techniques have allowed to overcome even Doppler broadening effects: it is in fact possible now to cool the atoms down to temperatures for which the Doppler linewidth is much smaller than the natural one.[3]

However, all these kinds of experiments require an apparatus that is far from being simple and portable: they need in fact several laser sources to manipulate the atoms and the alignment can be problematic. Since the recent progress in growing semiconductor samples with optical features sufficiently sharp and free from unwanted damping effects, there has been much interest in trying to export all the nonlinear and quantum optics formalism to the description of optical effects in solid-state samples. From the experimental point of view it is in fact much simpler to work with a solid-state sample: once it has been grown, in fact, there is no need for complicate manipulations but for its cooling down to a few Kelvin. Also for applications, it would be very useful to have optical elements as little and as portable as semiconductor ones; light-emitting diodes, harmonic generators, bistable elements are in fact widely applied in all sort of devices.

Also from a fundamental point of view the study of optical properties of solid-state materials can bring to a deeper understanding of the physics of both the underlying material and the electromagnetic field, which can be made to interact with material excitations of various kinds. In this sense heterostructures made up of different semiconducting materials allow for the possibility of having a quantization of carrier motion and thus open up the possibility of studying systems of reduced dimensionalities (quantum wells, wires and dots).[4] Nonlinear optical properties of such eminently quantum devices are very pronounced, since the confinement of carriers makes the excited electron-hole pairs to interact more strongly among them; in this way, it has been possible to observe sharp excitonic features in the susceptibilities and also a strong dependence of the response on the excitation level.[5,6]

Another possibility that has been opened up by the development of semiconductor structures consists in the modification of the structure of photonic modes in order to act either on the radiative linewidths of the transitions or, more relevantly, on the photonic eigenfunctions. In this way, it is possible to have either forbidden regions or sharp peaks in the photonic density of states, corresponding respectively to the gaps of a photonic band-gap crystal or to localized states.[4]

The realization of high finesse microcavities is a typical example of such techniques: the distributed Bragg reflectors (DBR) are in fact grown by epitaxial methods and consist in stacks of $\lambda/4$ layers of different refraction indices. In this way, the coupling of the material degrees of freedom to the radiative ones can be made strong enough to allow, e.g., the observation of exciton-photon strong coupling effects.[7] Both

the light and the carrier confinement, in fact, enhance the light-matter interaction.

Much of the published literature deals with the linear optics of semiconductor microcavities; only recently nonlinear and quantum effects in such structures have been studied and observed.[8–14] This field obviously deserves a greater attention, both because it can provide new informations on the dynamics of carriers in heterostructures and because the specific nonlinear properties of the material may allow for new effects.

The present paper is devoted to a detailed analysis of a pair of different systems, the mathematical description of which is however exactly identical. The first of them consists in a microcavity supporting two photonic modes at frequencies ω_1 and $\omega_2 \approx 2\omega_1$; assuming an appreciable *second harmonic generation* (SHG) in the material medium, the two photonic modes result nonlinearly coupled one to the other by a term that corresponds to efficient[14–17] mutual conversion of two fundamental photons into an harmonic photon and vice-versa. The second system consists in a microcavity supporting one photonic mode at a frequency ω_1 approximately equal to half the frequency ω_2 of an excitonic transition; if this latter allowes for *two-photon absorption* (TPA), the excitonic mode and the photonic mode result coupled by a term that converts two photons into an exciton and vice-versa.

After the general discussion of the model contained in Sec. II, Sec. III is devoted to the analysis of transmission spectra through our system when it is illuminated at a frequency approximately equal to the frequency of the lower mode. At linear regime the spectra are characterized by a single peak at the exact frequency of the lower mode ω_1, while at high intensities the main effect is either the appearance of a new peak at half the higher mode frequency $\omega_2/2$ or to a *two-photon Rabi splitting* in the resonant case ($\omega_1 \simeq \omega_2/2$).

Section IV is devoted to the linear optical response of our system when it is *dressed* by a strong pump beam; such a case is much similar to the usual optical Stark effect, in which an atomic transition is driven by a pump beam and probed by a weak probe beam.[18–20] Differently from that case, in which the nonlinearity was intrinsic in the two-level structure of the material excitation, we are now dealing with a pair of linear oscillators interacting with each other by means of a two-photon coupling term; for this reason we shall refer to it as a *two-photon optical Stark effect* (TPOSE).

Because of this similarity, our results are physically most interesting in the two-photon absorption case; hence we shall concentrate on the absorption spectra in the case the system is driven at a frequency near the lower photonic mode and probed near the upper excitonic mode. The main feature that we shall discuss is the strong dependence of probe absorption spectra on pump intensity. When the intensity of the pump is low enough, the spectra show a single excitonic peak; at moderate intensities, the dressing gives origin to another peak in addition to this one. At even higher intensities, the response is characterized by a more complex behavior and at particular frequencies the system gives even rise to some gain by means of stimulated hyper-Raman scattering processes.

To make the discussion complete, it is necessary to give an explicit expression for the coupling coefficient between the modes, starting from the experimentally accessible nonlinear optical susceptibilities $\chi^{(2)}$ and $\chi^{(3)}$. This is done in Sec. V, together with a numerical estimate of the light intensity needed for the actual experimental observations of two-photon Rabi splitting or two-photon optical Stark effect.

II. THEORETICAL MODEL AND GENERAL RESULTS

Consider a system with two bosonic degrees of freedom nonlinearly coupled by cubic interaction terms and driven by classical external fields:

$$H=\hbar\omega_1 b_1^\dagger b_1+\hbar\omega_2 b_2^\dagger b_2+\hbar\beta b_2^\dagger b_1^2+\hbar\beta^* b_1^{\dagger 2} b_2+\hbar k_1 E_1(t) b_1^\dagger+\hbar k_1^* E_1^*(t) b_1+\hbar k_2 E_2(t) b_2^\dagger+\hbar k_2^* E_2^*(t) b_2 . \quad (2.1)$$

Such a Hamiltonian,[21–25] supplemented by phenomenological damping terms, can describe a few different nonlinear optical effects: our attention will be concentrated upon the two cases of resonant two-photon absorption (TPA) and of doubly resonant second harmonic generation (SHG) inside a microcavity. In the TPA case one boson is a cavity photon and the other is an exciton, while in the SHG both bosons are cavity photons. The nonlinear coupling is supposed to be nearly resonating, i.e., $2\omega_1$ is supposed to be close to ω_2; apart from the inclusion of phenomenological damping terms, all other modes of the system will be neglected.

The intensity of the coupling, given by the β coefficient, is related to the second-order susceptibility $\chi^{(2)}(-2\omega_1;\omega_1,\omega_1)$ in the SHG case, or to the third-order one $\chi^{(3)}(-\omega;\omega,-\omega,\omega)$ in the TPA case. In Sec. V, we shall give an explicit expression for β and a rough estimate of its magnitude in the simplest physical configurations for GaAs-based microcavities.

The $\hbar k_i E_i(t) b_i^\dagger+\hbar k_i^* E_i^*(t) b_i$ terms describe the driving of the b_1 and b_2 modes by external classical fields $E_1(t)$ and $E_2(t)$, e.g., laser beams incident on the cavity: a photonic mode can be driven by the external light field which leaks into the cavity through the nonperfectly reflecting front mirror, while an excitonic mode can be driven by an external radiation provided the cavity mirrors are nearly transparent at its frequency, in order for the photonic mode structure of the cavity not to affect the (linear) coupling of the external radiation to the exciton. In the following, we shall simplify the notation by letting $F_i(t)=k_i E_i(t)$.

Because of the coupling to the continuum of external radiative modes, the eigenmodes of our system have a finite

lifetime and their energy is radiated out of the cavity as free photons. Since these effects are dissipative, they are not included in the Hamiltonian above, but they can be introduced phenomenologically in the equations of motions for the field amplitudes [see the $-\gamma_i b_i$ terms in the Eqs. (2.2) and (2.3) below]. But radiative broadenings are not the only possible ones: free pair absorption for photonic modes, phonon and disorder scattering or ionization for excitonic modes give additional contributions to the broadening parameters γ_i. Other possible forms of damping terms, which can arise, e.g., from two-photon free pair absorption or quantum coherence effects,[26] will not be considered in the following; however they could be necessary for a refined fit of experimental data.

In the classical limit $\langle b_1^\dagger b_1\rangle, \langle b_2^\dagger b_2\rangle \gg 1$ all operators can be replaced by their mean values (i.e., the mean value of any product of operators equals the product of the mean values) and the equations of motion for the field amplitudes can be written as:

$$\dot{b}_1 = -i\omega_1 b_1 - \gamma_1 b_1 - 2i\beta^* b_2 b_1^* - iF_1(t) \tag{2.2}$$

$$\dot{b}_2 = -i\omega_2 b_2 - \gamma_2 b_2 - i\beta b_1^2 - iF_2(t). \tag{2.3}$$

Such a description clearly does not take into account all those effects that arise from the quantum nature of the fields and their quantum and thermal fluctuations.[27,28]

Leaving aside subharmonic generation effects[23,29] that take place when the system is driven on the harmonic mode, we shall concentrate our attention on the case in which the driving is only on the fundamental mode and it is monochromatic at frequency ω_L: $F_1(t) = F_o e^{-i\omega_L t}$ and $F_2 = 0$. It is convenient to introduce the slowly varying variables $a_1 = b_1 e^{i\omega_L t}$ and $a_2 = b_2 e^{2i\omega_L t}$; putting $\delta_M = (\omega_2 - 2\omega_1)/2$ and $\delta_L = \omega_L - \omega_1$, the evolution of the system will be given by

$$\dot{a}_1 = i\delta_L a_1 - \gamma_1 a_1 - 2i\beta^* a_2 a_1^* - iF_o \tag{2.4}$$

$$\dot{a}_2 = 2i(\delta_L - \delta_M) a_2 - \gamma_2 a_2 - i\beta a_1^2. \tag{2.5}$$

A great deal of information about the physical behavior of our system can be obtained by looking for stationary solutions of the system of differential Eqs. (2.4) and (2.5); the system being dissipative, it can, in fact, be expected to generally converge to a stationary solution at least for weak drivings. In any case, the stability of the solution found can be verified by means of the usual linearization techniques.

The stationary solutions (A_1 and A_2) are given by the equations

$$A_1\left[\delta_L + i\gamma_1 - \frac{|\beta A_1|^2}{\delta_L - \delta_M + i\gamma_2/2}\right] = F_o \tag{2.6}$$

$$A_2 = \frac{\beta A_1^2/2}{\delta_L - \delta_M + i\gamma_2/2} \tag{2.7}$$

and the stability can be determined from the eigenvalues of the linearized system[21]

$$\frac{d}{dt}\delta\vec{\alpha} = \mathbf{M}\cdot\delta\vec{\alpha}, \tag{2.8}$$

where we have introduced the displacement from the steady-state solution

$$\begin{aligned}\delta\vec{\alpha} &= (a_1 - A_1, a_1^* - A_1^*, a_2 - A_2, a_2^* - A_2^*)^T \\ &= (\delta a_1, \delta a_1^*, \delta a_2, \delta a_2^*)^T\end{aligned} \tag{2.9}$$

and the linearized evolution matrix

$$\mathbf{M} = \begin{pmatrix} -\gamma_1 + i\delta_L & -2i\beta^* A_2 & -2i\beta^* A_1^* & 0 \\ 2i\beta A_2^* & -\gamma_1 - i\delta_L & 0 & 2i\beta A_1 \\ -2i\beta A_1 & 0 & -\gamma_2 + 2i(\delta_L - \delta_M) & 0 \\ 0 & 2i\beta^* A_1^* & 0 & -\gamma_2 - 2i(\delta_L - \delta_M) \end{pmatrix}. \tag{2.10}$$

III. TRANSMISSION AND SECOND HARMONIC GENERATION SPECTRA: TWO-PHOTON RABI SPLITTING

Such a simple theory can predict exactly the transmission properties of the structure: to visualize their behavior, in Fig. 1 we have reproduced a few spectra of the internal intensity parameter $\Omega^2 = |\beta A_1|^2$ (which is proportional to the internal intensity as well as to the transmitted one) as function of the driving frequency δ_L, for different values of incident (driving) intensity: the left panel refers to the exact resonance $\delta_M = 0$ case, the right panel to the detuned case $\delta_M = 4\gamma$. The whitened regions correspond to unstable behavior. We have supposed $\gamma_1 = \gamma_2 = \gamma$.

In the latter case ($\delta_M = 4\gamma$), the transmitted intensity at low-incident intensity, i.e., in the linear regime limit, is characterized by a single peak at $\delta_L = 0$ (i.e., at $\omega_L = \omega_1$); at higher intensities, a new peak appears close to $\delta_L = \delta_M$ (i.e., at $\omega_L \simeq \omega_2/2$) and for growing intensities the peaks bend in the external direction repelling each other and tend to have the same strength. In the $\delta_M = 0$ case, the transmitted intensity shows initially a single peak at $\delta_L = 0$, which at higher intensities splits in two; for growing intensities the two components bend again towards the external direction, their strengths staying equal.

Thanks to the bending of the transmission peaks with growing intensity, dispersive optical bistability can be obtained:[23] a multiple intersection of the vertical straight line

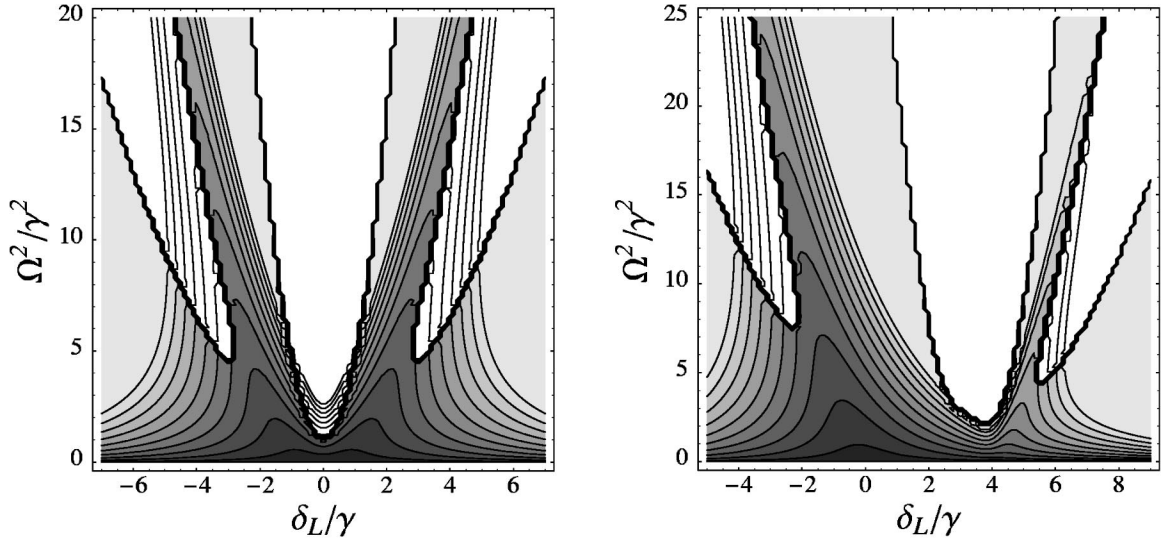

FIG. 1. Internal intensity parameter ($\Omega^2=|\beta A_1|^2$, proportional to the internal as well as to the transmitted intensity) for different values of (constant) incident intensity as a function of the detuning of the incident field δ_L. Left panel: exact resonance case $\delta_M=0$. Right panel: $\delta_M=4\gamma$. The grey scale corresponds to the incident intensity: lighter shadowing means higher intensity; white regions correspond to unstable behavior.

corresponding to a given δ_L with the transmission spectrum at a given incident intensity has the physical meaning of optical multistability.[10,30] The instability region present under the bended peak correspond to the central unstable branch of the hysteresis loop. The instability predicted in the region between the two peaks correspond instead to a so-called hard-mode transition: the eigenvalues of the stability matrix **M** having a nonvanishing imaginary part at the threshold, the system goes from a stable solution to a limit cycle, which physically corresponds to selfpulsing of the transmission with time.[21,23,25]

The intensity of the generated harmonic field is proportional to $I_h=|A_2|^2$; from Eq. (2.7) it follows that it is proportional to the square of the fundamental mode internal intensity times a *temporal phase-matching* factor $(\delta_L-\delta_M+i\gamma_2/2)^{-1}$, whose physical meaning will be clarified in the following. In Fig. 2 we have represented the spectra of harmonic intensity as function of the incident frequency δ_L, for different values of incident intensity; again the left panel corresponds to the exact resonance $\delta_M=0$ case, while the right panel to the detuned $\delta_M=4\gamma$ case. As done previously, instability regions have been whitened. The principal features are analogous to the previously analyzed transmission case: optical bistability and self pulsing can be observed also by looking at the harmonic-field intensity; this last remark is most important in the SHG case, where the efficiency of the harmonic generation can be affected by these effects (see, e.g., Fig. 3 of Ref. 17).[17] Notice the typical quadratic dependence of the harmonic intensity on the *internal* fundamental intensity: all the bistability and selfpulsing

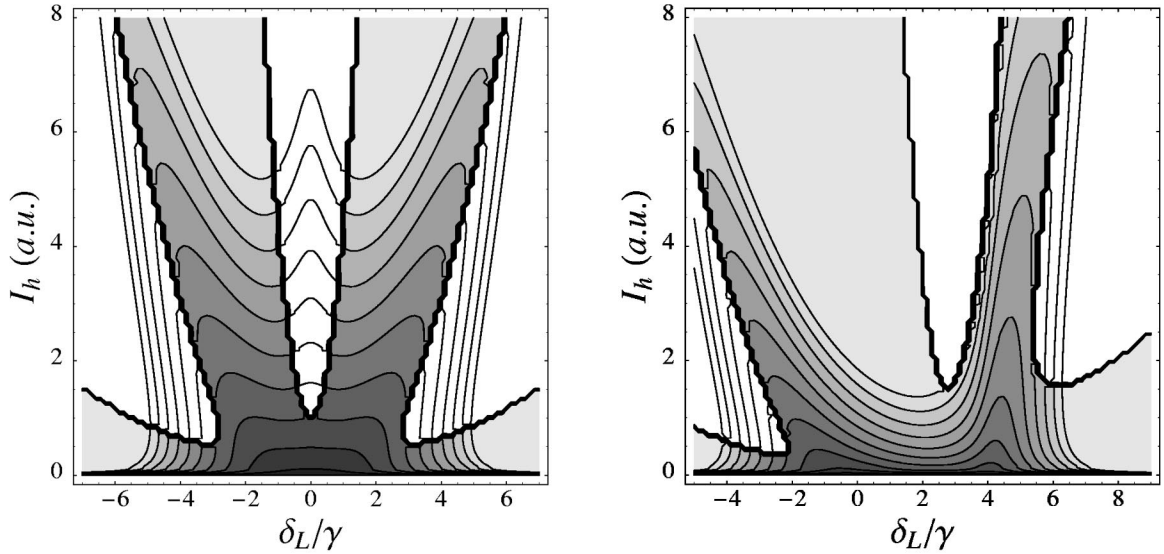

FIG. 2. Second harmonic intensity spectra for different values of (constant) incident intensity. Left panel: exact resonance case $\delta_M=0$. Right panel: $\delta_M=4\gamma$. The grey scale corresponds to the incident intensity: lighter shadowing means higher intensity; white regions correspond to unstable behavior.

effects are in fact due to the coupling of the incident beam with the cavity mode at the fundamental frequency.

A. Physical interpretation of the results

The relatively simple structure of Eq. (2.6) allows for a clear physical interpretation of the spectra of Fig. 1; since the transmittivity of the system τ is proportional to the ratio of the internal amplitude A_1 and the incident amplitude F_o, we can focus our attention on its rescaled version

$$\tilde{\tau}=\frac{A_1}{F_o}=\left[\delta_L+i\gamma_1-\frac{\Omega^2}{\delta_L-\delta_M+i\gamma_2/2}\right]^{-1}. \tag{3.1}$$

The dependence of the transmittivity τ on the transmitted intensity Ω^2 is a typical signature of nonlinear effects: for the moment we shall consider Ω as an independent parameter and we shall study the behavior of the transmission spectrum at fixed Ω.

Neglecting for the sake of simplicity the damping terms $\gamma_{1,2}$, the transmitivity (as function of laser frequency δ_L) has two closely spaced poles located at

$$\delta_{1,2}=\left[\frac{\delta_M}{2}\pm\left(\frac{\delta_M^2}{4}+\Omega^2\right)^{1/2}\right]; \tag{3.2}$$

whose weights are redistributed according to the equations

$$f_1=\frac{\delta_1-\delta_M}{\delta_1-\delta_2} \tag{3.3}$$

$$f_2=\frac{\delta_2-\delta_M}{\delta_2-\delta_1}, \tag{3.4}$$

the total strength f_1+f_2 being constant and equal to 1.

These results are easily interpreted in the two-level system framework[29] as a nonlinear Rabi splitting of two quasiresonant states, detuned of $2\delta_M$ and coupled to each other through the intensity dependent Ω term. We refer to it as *two-photon* Rabi splitting because it is due to the cubic interaction term $\hbar\beta b_2^{\dagger}b_1^2+\text{H.c.}$ At linear regime, i.e., when the coupling is vanishing, one eigenstate corresponds to a pair of photons in the fundamental mode and the other to a single boson on the harmonic mode; clearly only the former is *bright* in a transmission experiment at low intensity. At higher intensities, when the nonlinear interaction begins to be important, the modes are mixed up and the bright component is redistributed among them. Thanks to such a redistribution, the spectrum start to show a pair of peaks: the stronger one is initially at ω_1, while the weaker one appears at $\omega_2/2$ (the factor 1/2 accounts for the fact that *two* fundamental bosons must be destroyed to create an harmonic one). For growing coupling Ω their mutual interaction make them repel in energy and equalize in strength; at very high intensities, the detuning δ_M becomes small as compared with the coupling Ω and thus we have a doublet of equally strong peaks with a splitting equal to 2Ω [we can neglect δ_M in Eq. (3.2)]. When $\delta_M=0$ the poles are equally bright at any intensity, since the resonance condition guarantees an equal distribution of the bright component. Moreover the two peaks are symmetrically placed with respect to $\omega_1=\omega_2/2$ with a splitting equal to 2Ω.

So far, we have studied the transmittivity spectrum as it depends on the parameter Ω: in physical terms we have studied the transmission properties at fixed transmitted intensity. The experimentally relevant spectra are however the ones in which the incident intensity is kept constant; this calculation requires an inversion of the functional relation between the incident intensity and the transmitted intensity. The curves of Figs. 1 and 2 have been plotted after performing such an inversion, the sawtooth appearance of the instability being due to finite numerical resolution.

B. Comparison with another quadratically nonlinear system

The Eqs. (2.4) and (2.5), which describe the time evolution of our system, are very similar to the ones describing spatial propagation of a monochromatic wave through a second harmonic generating medium when the undepleted pump approximation is not made. If we denote E_ω and $E_{2\omega}$, the slowly varying field amplitudes respectively of the fundamental and the harmonic field, n_ω and $n_{2\omega}$ the refraction indices and Δk the wave-vector mismatch $2k_\omega-k_{2\omega}$ and we switch to the new variable $\hat{E}_{2\omega}=(1/\sqrt{2})E_{2\omega}e^{-i\Delta kz}$, the propagation equations in the so-called slowly varying envelope approximation (SVEA) have the form[6]

$$\frac{\partial}{\partial z}E_\omega=\frac{i\omega\sqrt{2}}{2n_\omega c}[\chi^{(2)}(-2\omega;\omega,\omega)E_\omega^*\hat{E}_{2\omega}]-\gamma_1E_\omega \tag{3.5}$$

$$\frac{\partial}{\partial z}\hat{E}_{2\omega}=\frac{i\omega\sqrt{2}}{2n_{2\omega}c}\left[\frac{1}{2}\chi^{(2)}(-2\omega;\omega,\omega),E_\omega^2\right]-i\Delta k\hat{E}_{2\omega}-\gamma_2\hat{E}_{2\omega}, \tag{3.6}$$

which have the same formal structure as Eqs. (2.4) and (2.5), apart from the forcing term E_o; in particular the wave-vector mismatch Δk plays the role of the mode detuning $2\delta_M$; for this reason the factor $(\delta_L-\delta_M+i\gamma_2/2)^{-1}$ above is responsible for the temporal phase matching: at a given fundamental (internal) intensity, the amplitude of the generated harmonic field is proportional to the inverse of the mismatch, i.e., the coherence time. Of course, despite the mathematical similarity of the equations, the physical informations which have to be extracted is different: in the present case, we are looking for the steady state in presence of driving terms, while in the case of Eqs. (3.5) and (3.6) the driving term is absent and boundary conditions at the interfaces of the nonlinear slab have to be imposed.

IV. TWO-PHOTON OPTICAL STARK EFFECT: PROBING THE DRESSED SYSTEM

In the previous section we have described the steady-state response to a monochromatic strong driving and we have focused on stable equilibria, at the expense of other features, like selfpulsing. The stability of such solutions has been verified checking that all the eigenvalues of the linearized evolution matrix **M** have negative real part. But the linearized theory can also give a lot of other information on the dynamical behavior of the system when it is illuminated by a strong beam: besides quantum fluctuation effects in the spectra of transmitted and sub/second harmonic light, which have been already studied in detail by Drummond *et al.*,[24] the lin-

earized evolution can be used to determine the (linear) response of this *dressed* system to weak additional *probe* fields; the response of our system to the probe will in fact be different according to the intensity of the pump beam. Such an analysis is clearly restricted to pump intensities and frequencies that lie inside the stability region. The result we shall obtain are strictly related to Drummond's ones, since the general linear response theory connects the response of a system to its fluctuations (fluctuation-dissipation theorem[31]).

Calling again $\delta\vec{\alpha}$ the displacements of the slowly varying field amplitudes from the steady-state (in the absence of the probe) and $\mathbf{M}$ the linearized evolution matrix in the rotating frame [see Eqs. (2.9) and (2.10)], the equations of motion can be written as

$$\frac{d}{dt}\delta\vec{\alpha}=\mathbf{M}\cdot\delta\vec{\alpha}+\vec{f}(t), \tag{4.1}$$

where the $\vec{f}(t)$ term accounts for the probe field (again in the rotating frame) and corresponds to additional driving terms in Eqs. (2.4) and (2.5).

The solution of Eq. (4.1) is immediately obtained in the most simple case of a monochromatic driving term $\vec{f}(t)=\vec{f}_o e^{-i\omega t}$. Putting $\delta\vec{\alpha}(t)=\delta\vec{\alpha}_o e^{-i\omega t}$, it is easy to verify that

$$\delta\vec{\alpha}_o=-[\mathbf{M}+i\omega\mathbf{1}]^{-1}\cdot\vec{f}_o, \tag{4.2}$$

in this way the eigenvalues of $\mathbf{M}$ get the physical meaning of frequencies of the *dressed* modes of the system as driven by the pump beam: since $\mathbf{M}$ depends on the pump intensity F_o via the fields A_1 and A_2 that the pump generates inside the structure, the energies of the dressed modes and their weights (i.e., their oscillator strengths) will depend on the pump intensity as well. So the spectral features of the response to the probe beam will suffer remarkable qualitative changes when the pump intensity is varied. Without the cubic interaction term $\hbar\beta b_2^\dagger b_1^2+\text{H.c.}$ in the Hamiltonian, this effect would not be present and the response would be independent of the presence of the pump beam F_o.

Effects of this kind, which involve nonlinear interactions between a strong dressing (pump) beam and a weak probe have been the subject of active study for a couple of decades, but the interest has been for the greatest part focused on the intrinsic nonlinearities of two- or three-level atoms. The Mollow triplet of fluorescence[32,33] and the stimulated emission and absorption line shapes of nearly resonantly driven two-level atoms (optical Stark effect, OSE) (Refs. 18–20) are among the most celebrated examples. Very recently, there has been much interest on excitonic Mollow spectra in semiconductor microcavities: both experimental[12] and theoretical[13] work has been devoted to the observation of changes in the probe absorption spectrum when the exciton is resonantly dressed. Such an effect stems from the fermionic nature of the electron-hole pair forming the exciton, in the sense that at high-excitation densities the exciton cannot be considered a true boson anymore.[5,34] In the present paper we are considering a somewhat different case: instead of dealing with an intrinsically nonlinear material excitation, the nonlinearity is now concentrated in the mutual interaction between two rigorously bosonic modes. The predicted effect in the TPA case, in particular, does not require any deviation of the exciton from bosonic behavior,[13] but only the possibility of two-photon absorption excitation; for this reason it will be called *two-photon* optical Stark effect (TPOSE).

A most interesting quantity which can be calculated by means of this linear response theory is the excitonic polarization created in a TPA configuration by a weak-probe (test) field at a frequency ω_t close to ω_2: depending on the intensity F_o and the frequency ω_L of the pump, its spectral features can be radically different. For simplicity, we shall suppose that the cavity mirrors do not confine light at ω_2, so that the coupling of the exciton to the incident probe beam is not affected by the photonic mode structure of the cavity. An experimental observation of such effects clearly requires some violation of parity selection rules, in a way to make the excitonic transition allowed for both one-photon and two-photon absorption: a single quantum well under a strong static electric field perpendicular to the quantum well layers[35] or an asymmetric quantum well[36–38] structures could be good choices.

In the slow variables, the additional driving term corresponding to the probe has the form

$$\vec{f}(t)=iF_t\begin{pmatrix}0\\0\\1\\0\end{pmatrix}e^{-i(\omega_t-2\omega_L)t}-iF_t^*\begin{pmatrix}0\\0\\0\\1\end{pmatrix}e^{i(\omega_t-2\omega_L)t}, \tag{4.3}$$

we have set $F_t=k_tE_t$ where E_t is the amplitude of the probe beam and k_t is a coupling coefficient proportional to the dipole matrix element of the one-photon transition. In the following we shall also use the reduced probe frequency defined as $\delta_t=\omega_t-2\omega_L$. The polarization of the system is determined by the third element of the response δa_2. Since the additional driving term contains two different frequencies $\pm\delta_t$, the response of the system will also have two spectral components

$$\delta\vec{\alpha}(t)=\delta\vec{\alpha}^{(+)}e^{-i\delta_t t}+\delta\vec{\alpha}^{(-)}e^{+i\delta_t t}, \tag{4.4}$$

which result in an actual excitonic polarization oscillating at both ω_t and $4\omega_L-\omega_t$

$$\begin{aligned}P_{exc}(t)&=\{\delta a_2^{(+)}e^{-i\delta_t t}+\delta a_2^{(-)}e^{i\delta_t t}\}e^{-2i\omega_L t}+\text{H.c.}\\&=\{\delta a_2^{(+)}e^{-i\omega_t t}+\delta a_2^{(-)}e^{-i(4\omega_L-\omega_t)t}\}+\text{H.c.}\end{aligned} \tag{4.5}$$

The first term derives from the linear polarization of the (dressed) system and has the same frequency ω_t as the forcing field; the second term instead describes a polarization at a frequency, which is symmetrical of ω_t with respect to the oscillation frequency $2\omega_L$ of the dressing field A_2. This last term, which is present in atomic systems as well, arises from nonlinear wave-mixing effects of the (weak) probe with the (strong) pump beam.

The expression (4.5) for the polarization can be rearranged as

$$P_{exc}(t)=e^{-i\omega_t t}\{\delta a_2^{(+)}+\delta a_2^{(-)}e^{2i\delta_t t}\}+\text{H.c.}; \tag{4.6}$$

physically this means that the resulting polarization can be seen as an oscillating polarization at ω_t amplitude modulated at δ_t. Since the modulation frequency δ_t is generally rather high, the most relevant quantity is the *mean* absorption suffered by the probe beam, and then only the first term in brackets $\delta a_2^{(+)}$ must be retained. The susceptibility is then given by $\chi_{exc} \propto \delta a_2^{(+)}/E_t$ and probe absorption is proportional to its imaginary part.

Its most peculiar physical features can be predicted in a rather simple way by looking at the explicit form of the equation of motion for the actual (not the slowly varying) displacements of the fields from equilibrium $\delta b_1, \delta b_1^*, \delta b_2$, and δb_2^* [cf. Eqs. (2.2) and (2.3)]

$$\delta \dot{b}_1 = -i\omega_1 \delta b_1 - \gamma_1 \delta b_1 - 2i\beta^* A_1^* e^{i\omega_L t} \delta b_2 - 2i\beta^* A_2 e^{-2i\omega_L t} \delta b_1^* \tag{4.7}$$

$$\delta \dot{b}_2 = -i\omega_2 \delta b_2 - \gamma_2 \delta b_2 - 2i\beta A_1 e^{-i\omega_L t} \delta b_1 + iF_t e^{-i\omega_t t} \tag{4.8}$$

$$\delta \dot{b}_1^* = i\omega_1 \delta b_1^* - \gamma_1 \delta b_1^* + 2i\beta A_1 e^{-i\omega_L t} \delta b_2^* + 2i\beta A_2^* e^{2i\omega_L t} \delta b_1 \tag{4.9}$$

$$\delta \dot{b}_2^* = i\omega_2 \delta b_2^* - \gamma_2 \delta b_2^* + 2i\beta A_1^* e^{i\omega_L t} \delta b_1^* - iF_t^* e^{i\omega_t t}; \tag{4.10}$$

two different sorts of time-dependent coupling terms are present: the first one, whose intensity is proportional to $\Omega = |\beta A_1|$, connects the δb_1 and δb_2 fields to each other; the other one, whose intensity is instead proportional to $|\beta A_2|$ and thus to Ω^2, connects the δb_1 field to its complex conjugate δb_1^*.

For moderate pump intensities only the former one will be important and thus the pair of fields $\delta a_{1,2}$ will be decoupled from the complex conjugate fields $\delta a_{1,2}^*$. From the numerical calculations, it results that the fields and their conjugates are effectively decoupled only for pump intensities below the instability regions. If we neglect the latter coupling (i.e., the one $\propto |\beta A_2|$), the system can be described as a pair of linearly coupled oscillators at ω_1 and ω_2 with a time-dependent coupling term $-2i\beta A_1 e^{-i\omega_L t}$; by setting $\delta \tilde{b}_1 = e^{-i\omega_L t} \delta b_1$, the time dependence of the coupling term can be eliminated: in this way, the equations of motion (4.7) and (4.8) can be simply rewritten as

$$\delta \dot{\tilde{b}}_1 = -i(\omega_1 + \omega_L)\delta \tilde{b}_1 - \gamma_1 \delta \tilde{b}_1 - 2i\beta^* A_1^* \delta b_2 \tag{4.11}$$

$$\delta \dot{b}_2 = -i\omega_2 \delta b_2 - \gamma_2 \delta b_2 - 2i\beta A_1 \delta \tilde{b}_1 + iF_t e^{-i\omega_t t}. \tag{4.12}$$

The eigenmodes of this system depend on the bare frequencies $\omega_1 + \omega_L$ and ω_2 and the coupling $-2i\beta A_1$ in the usual way for a two-level system: a pair of modes at frequencies ω_α and ω_β that start respectively at $\omega_1 + \omega_L$ and ω_2 and tend to mix and repel as the intensity of the coupling grows up. Since the driving is only on the second mode, at low-coupling intensity the brightness is concentrated in this mode, while for growing intensity it tends to redistribute equally among both eigenmodes. The probe absorption spectra will show peaks at the oscillation frequencies of the modes and the intensity of each peak will be proportional to its brightness.

Figures 3 and 4 contain two series of spectra that differ from each other for the choice of detuning parameters δ_L and δ_M: in each series the absorption spectra are plotted as a function of probe frequency at growing dressing intensities A_1 (and hence couplings); the frequency zero has been set at the excitonic frequency ω_2. Consider the first spectrum, reproduced in the upper left panel of Fig. 3 ($\delta_M/\gamma = -2$ and $\delta_L/\gamma = 8$): at very low-dressing intensity (a), we recover the linear spectrum, with a single peak at the frequency of the bare excitonic mode ω_2; at slightly higher intensity (b) a new peak appears at a frequency $\omega_t = \omega_1 + \omega_L$ [i.e., $(\omega_t - \omega_2)/\gamma = (\delta_L - 2\delta_M)/\gamma = 12$]; as intensity grows up (c) and (d) the strengths of these two peaks tend to equalize and their energies to repel each other. This is a clear signature of mixing and repelling of two (one dark and one bright) coupled modes in a two-level system.

The physical meaning of the peak at $\omega_1 + \omega_L$ instead of $2\omega_1$ can be understood if we think at the nature of the oscillating coupling; this is in fact due to the dressing field $A_1 e^{-i\omega_L t}$ and in quantum terms it converts an exciton in the harmonic (ω_2) mode into a photon in the fundamental (ω_1) mode plus one more photon in the dressing field. Different from the previously analyzed single beam nonlinear optics, the coupling is now linear in the fields $\delta b_{1,2}$, so that the spectral features do not depend on the intensity of the probe beam, provided this is weak enough not to perturb appreciably the system. This is again due to the fact we are not dealing anymore with the conversion of one harmonic boson in two fundamental ones, as we were doing in the one-beam case, but with a conversion of a harmonic exciton into a single fundamental photon plus a dressing A_1 photon (ω_L).

Analogous considerations can be repeated in order to explain the structure of the spectrum reproduced in the upper left panel of Fig. 4 ($\delta_L/\gamma = 6$ and $\delta_M/\gamma = 3$), though the resonance condition $\omega_2 = \omega_1 + \omega_L$ makes the spectra look somewhat different: the bare modes at ω_2 and $\omega_1 + \omega_L$ are in fact resonant and hence the coupling does not introduce a new peak, but only split the existing one in a symmetric doublet of peaks. This is still centered at $\delta_t = 0$ and its spacing grows with growing dressing field intensity.

As it can be observed in the upper right panels of Figs. 3 and 4, at higher pump intensities the $-2i\beta^* A_2 e^{-2i\omega_L t}$ coupling terms start to be relevant as well. In particular, its effect begins to be dramatic when one of the absorption peaks (the upper one at ω_α, in our specific cases) is close to $2\omega_L$ (i.e., $\omega_t - \omega_2 = 2\delta_L - 2\delta_M$), frequency at which it resonates. This is verified when the dressing intensity is close to the lower edge of the bistability unstable region. In this case, the peak narrows (the threshold corresponds to the vanishing of the real part of one eigenvalue of **M**), its shape is modified and some gain (i.e., negative absorption) appears [see spectra (e)] at a frequency just above the resonance frequency $2\omega_L$.

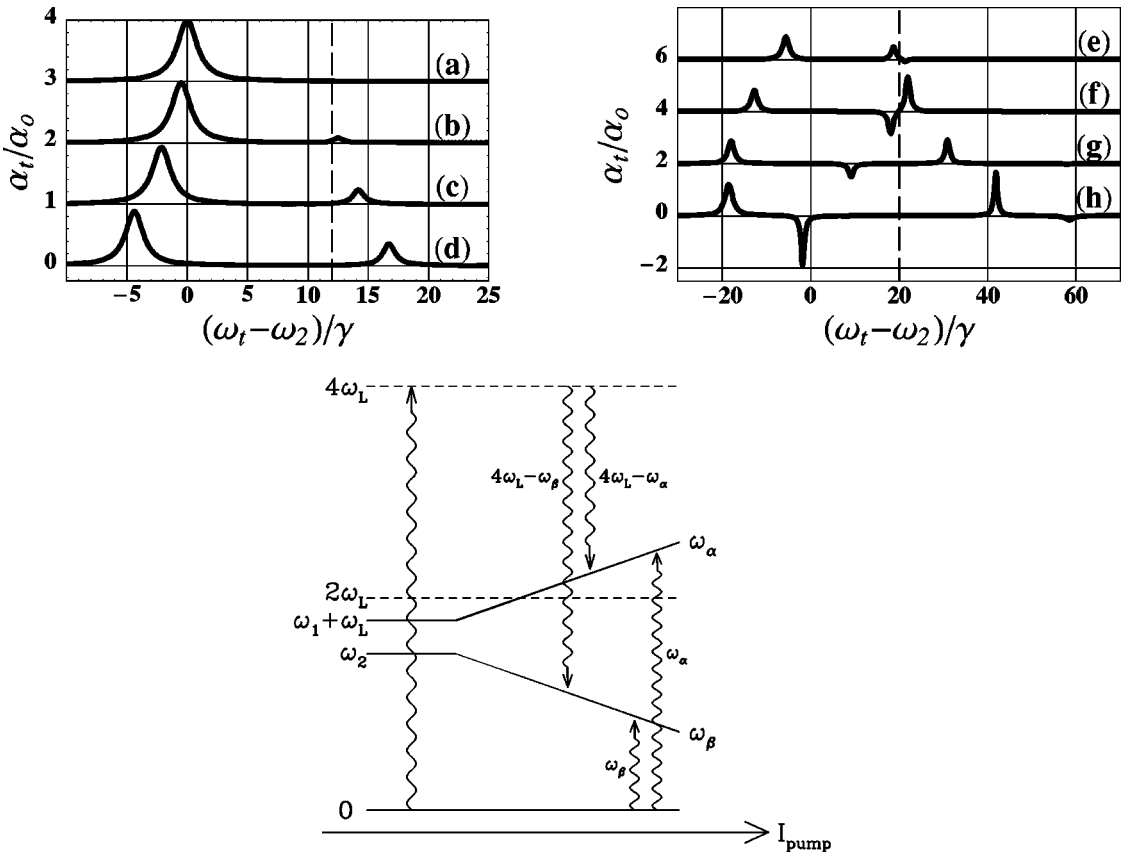

FIG. 3. In the two upper frames, probe absorption spectra at different dressing intensities. Absorption has been normalized to the bare exciton absorption. Dressing intensity grows from (a) to (h); instabilities are between (e) and (f) and above (h). Notice the change of frequency scale. Nonresonant case $\omega_1+\omega_L-\omega_2=12\gamma$, $2\omega_L-\omega_2=20\gamma$: $\delta_M/\gamma=-2$, $\delta_L/\gamma=8$. In the lowest frame, schematic plot of the energy levels involved in the optical processes: the frequencies ω_α and ω_β of the dressed states shift with increasing pump intensity.

Increasing the dressing intensity above the bistability unstable region, i.e., in the upper branch of the hysteresis curve, the spectra result radically different. The two absorptive peaks are still present at frequencies ω_α and ω_β and keep on repelling themselves as the pump intensity grows up. At the same time, a gain peak is present at a frequency $4\omega_L-\omega_\alpha$, which is the symmetric of the upper absorption peak frequency ω_α with respect to the resonance frequency $2\omega_L$. For growing pump intensity, as the absorption peak frequency ω_α shifts towards higher frequencies because of the coupling term $-2i\beta A_1 e^{-i\omega_L t}$, the gain peak shifts towards lower frequencies in order to satisfy the symmetry condition with respect to $2\omega_L$. Near the threshold of the self-pulsing instability, the other absorptive peak at ω_β begins to have a gain counterpart at $4\omega_L-\omega_\beta$ as well: in Fig. 3 this gain peak is hardly visible near $(\omega_t-\omega_2)/\gamma\simeq 60$, while in Fig. 4 it is located near $(\omega_t-\omega_2)/\gamma\simeq 20$.

Such qualitatively new features, are stable with respect to variations of detunings and linewidths as we have verified; in analogy to the gain appearing in the classical OSE,[1,19,20] a simple physical interpretation can be put forward in terms of stimulated hyper-Raman scattering[39] in a dressed system picture; the main effect of the $-2i\beta^* A_2 e^{-2i\omega_L t}$ coupling term is in fact to induce conversion of a few quanta of the dressing fields A_1 and A_2 (for a total frequency $4\omega_L$) into a dressed excitation (at ω_α or ω_β) plus one more photon in the probe beam (at ω_t), which thus results amplified. Indeed, for such a process, energy conservation imposes that $\omega_t=4\omega_L-\omega_{\alpha,\beta}$: in this way it is possible to explain the symmetry condition empirically found in the calculated spectra.

In order to understand why the hyper-Raman process takes place involving the $4\omega_L$ frequency, it is useful to reformulate the dynamics of the dressed system in the usual Hamiltonian formalism of quantum optics; in terms of the field displacements δb_1 and δb_2, the effective Hamiltonian of the (dressed) system can be written as

$$H_d=\hbar\omega_1\delta b_1^\dagger\delta b_1+\hbar\omega_2\delta b_2^\dagger\delta b_2+2\hbar\beta A_1 e^{-i\omega_L t}\delta b_2^\dagger\delta b_1+2\hbar\beta^* A_1^* e^{i\omega_L t}\delta b_1^\dagger\delta b_2+\hbar k_t E_t e^{-i\omega_t t}\delta b_2^\dagger+\hbar k_t^* E_t^* e^{i\omega_t t}\delta b_2$$
$$+\hbar\beta^* A_2 e^{-2i\omega_L t}\delta b_1^{\dagger 2}+\hbar\beta A_2^* e^{2i\omega_L t}\delta b_1^2. \qquad (4.13)$$

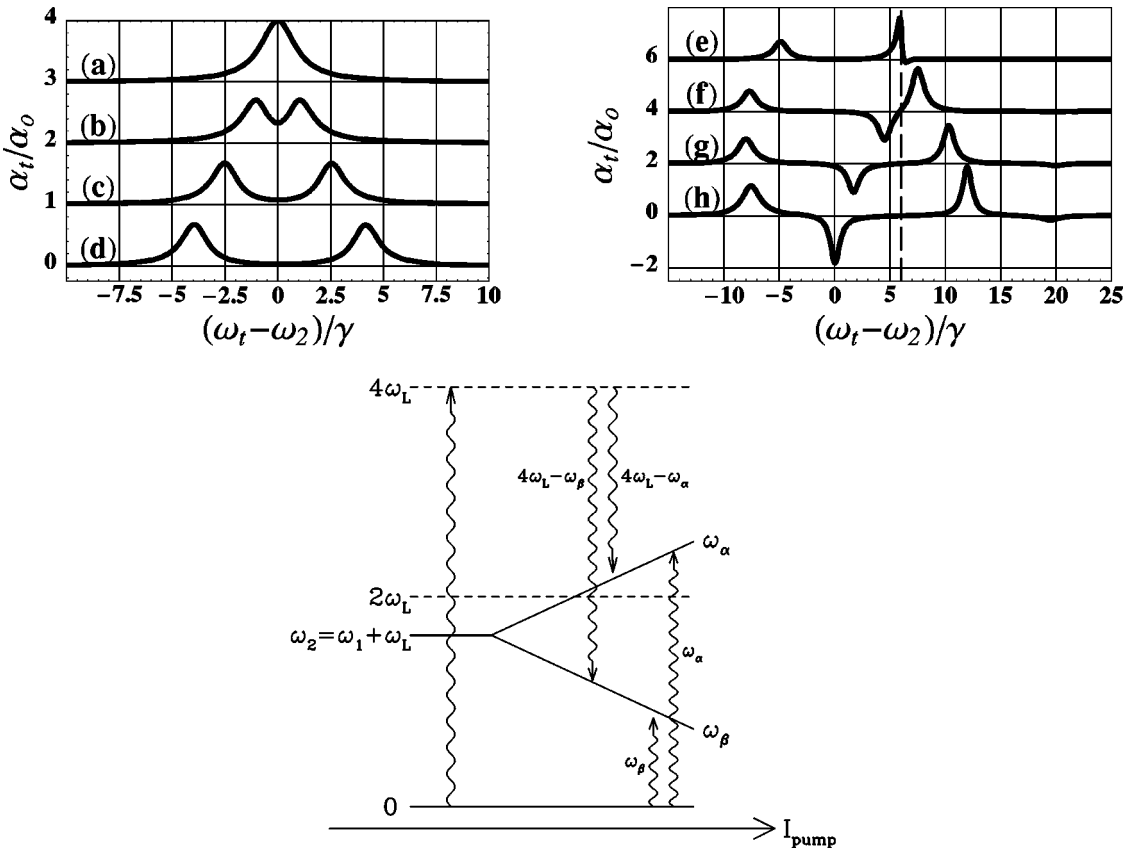

FIG. 4. In the two upper frames, probe absorption spectra at different dressing intensities. Absorption has been normalized to the bare exciton absorption. Dressing intensity grows from (a) to (h); instabilities are between (e) and (f) and above (h). Notice the change of frequency scale. Resonant case $\omega_1+\omega_L=\omega_2$, $2\omega_L-\omega_2=6\gamma$: $\delta_M/\gamma=3$, $\delta_L/\gamma=6$. In the lowest frame, schematic plot of the energy levels involved in the optical processes: the frequencies ω_α and ω_β of the dressed states shift with increasing pump intensity.

If we neglect for the moment the last two terms, we are left with two bosonic modes, linearly coupled to each other; this approximation is valid at low pump intensity, i.e., when the A_1 coupling is much greater than the A_2 coupling. As previously described, the probe absorption spectra are in this case characterized by a pair of absorptive peaks corresponding to the dressed modes at ω_α and ω_β, which result from diagonalization of the Hamiltonian.

The appearance of gain at higher pump intensities is due to the last two terms, which allow for the conversion of one harmonic dressing exciton A_2 at $2\omega_L$ into a pair of quanta of the fundamental mode $\delta b_1'$ and $\delta b_1''$ of frequencies respectively equal to ω_1' and ω_1''. One of these quanta then merges with a A_1 dressing photon at ω_L into an excitation at ω_α or ω_β, which is left inside the system; the other one, together with a A_1 dressing photon, is instead converted into an additional photon in the probe beam at ω_t. In conclusion, two A_1 dressing photons and one A_2 dressing exciton (for a total frequency equal to $4\omega_L$) are converted into a dressed excitation at ω_α or ω_β, plus a probe beam photon at ω_t: this kind of optical process, in which some quanta of a strong pump beam are scattered into an excitation of the material system plus an escaping photon, is called *hyper-Raman scattering*;[6] furthermore, since the emission of the escaping photon is stimulated by the probe beam, we shall say it is a *stimulated* hyper-Raman scattering.

As a final remark, it is interesting to notice that the sum rules demonstrated at all orders of perturbation theory in Ref. 40 are well verified even by our model, which allows for non-perturbative nonlinear optical effects, like optical bistability and optical selfpulsing; in particular the absorption sum rule, which states that the integral of the probe absorption coefficient over all frequency is independent of pump intensity, has been numerically verified in the stability regions. According to this sum rule the appearance of gain in some spectral region must compensates for an increased absorption in other spectral regions.

V. DISCUSSION OF MATERIAL AND GEOMETRICAL PARAMETERS

Until now, we have not paid attention to the absolute value of the nonlinear coupling β; all the effects described in the previous sections depend only on the product $\Omega=|\beta A_1|$. Indeed it seems theoretically possible to compensate for a small β by the use of high intensities; however very high-light intensities are not handy because of high-heat production inside the structure and the possibility of other competing nonlinear effects. A high β would thus allow for the observation of our specific two-photon processes at intensities at which other processes, like nonresonant Kerr nonlinearities, exciton bleaching or higher harmonic generation are negligible.

An explicit calculation of the parameter β can be performed starting from the usual optical constants of the materials forming the structure; as we have already pointed out, in

the SHG configuration β is related to the $\chi^{(2)}$ susceptibility of the materials, while in the TPA case it depends on the generalized oscillator strength of the two-photon absorptive transition, or, in other words, on the $\chi^{(3)}$ susceptibility. In the following, we limit our attention to planar structures, in which all the equations reduce to one-dimensional ones; the general case does not introduce in principle new different features, apart from the geometrical complications due to the vectorial character of the fields and the tensorial character of the susceptibilities.

If we expand the electromagnetic field in eigenvectors of the wave equation in a linear refractive background medium of dielectric constant $\epsilon(x)$

$$E(x,t)=\sum_i \{\mathcal{E}_i(x)e^{-i\omega_i t}a_i(t)+\mathcal{E}_i^*(x)e^{i\omega_i t}a_i^\dagger(t)\} \tag{5.1}$$

and we perform the so-called SVEA approximation, which correspond to supposing the temporal variation of the mode amplitudes to be much slower than the oscillation frequency, we get to the explicit expression for the coupling constant β in the SHG case[17]

$$\beta_{SHG}=-\frac{1}{\hbar}\int \mathcal{E}_2(x)^*\chi^{(2)}(x)\mathcal{E}_1(x)^2dx. \tag{5.2}$$

The physical interpretation of such an expression is evident: it is the overlap integral of the square of the fundamental wave function with the harmonic wave function weighted by the $\chi^{(2)}$ nonlinear susceptibility of the material; in a quantum field theoretical language, this expression corresponds to the matrix element of a three-photon vertex in which two fundamental photons annihilate into a harmonic photon. Since we are dealing with planar structures, the wave-function normalization has been chosen to be the natural one-dimensional one, i.e.,

$$\int \frac{\epsilon(x)}{2\pi}\mathcal{E}_i(x)^*\mathcal{E}_j(x)dx=\delta_{i,j}\hbar\omega_i; \tag{5.3}$$

in this way the mode intensities $|b_i|^2$ have the meaning of mean photon density per unit surface. From this choice it follows that the photonic wave function has the dimensions of an electric field times a length while β is the product of a frequency times a length. From Eq. (5.2) it is evident how the arbitrariness in the definition of the global phase of the wave functions reflects on the nonlinear coupling β (and analogously on the external couplings $k_{1,2}$): a change in the phase definition of the wave functions must in fact correspond to a change in the system parameters in a way to leave the Hamiltonian invariant.

In the presence of an isolated two-photon absorption transition, the $\chi^{(3)}$ susceptibility can be written as[6]

$$\chi^{(3)}(-\omega;\omega,-\omega,\omega)=\frac{f^{(3)}}{\hbar(\omega_2-2\omega-i\gamma_2)}; \tag{5.4}$$

because of its similarity with the well-known oscillator strength of a linear transition, the quantity $f^{(3)}$ can be called generalized oscillator strength of a (two-photon) transition. The nonlinear excitonic polarization can be written as

$$P_{NL}(x,t)=3e^{-i\omega_L t}\chi^{(3)}(x)|\mathcal{E}_1(x)|^2\mathcal{E}_1(x)|a_1|^2a_1. \tag{5.5}$$

Inserting this result in Maxwell's equations and performing the SVEA approximation as previously, we get to a motion equation for the field amplitude of the form

$$\frac{\partial a_1}{\partial t}=-\gamma_1 a_1-iF_o e^{-i(\omega_L-\omega_1)}+i\frac{3|a_1|^2a_1}{\hbar^2(\omega_{exc}-2\omega_L-i\gamma_{exc})}\int |\mathcal{E}_1(x)|^4 f^{(3)}(x)dx. \tag{5.6}$$

Comparing these term with the analogous equation that can be derived from our Hamiltonian formalism

$$\frac{\partial a_1}{\partial t}=-\gamma_1 a_1-iF_o e^{-i(\omega_L-\omega_1)}+i\frac{2|\beta|^2}{\omega_2-2\omega_L-i\gamma_2}|a_1|^2a_1 \tag{5.7}$$

we get to the final result

$$|\beta_{TPA}|^2=\frac{3}{2\hbar^2}\int |\mathcal{E}_1(x)|^4 f^{(3)}(x)dx; \tag{5.8}$$

the phase of β, which is still undetermined, is not physically important, since it determines only the relative phase of the fundamental and harmonic fields [see, e.g., Eq. (2.7)]; when we are driving the system on both modes, the phase of β fixes the phase of the amplitude oscillations in the excitonic polarization (4.6). The physical meaning of the remaning indetermination in the phase of β_{TPA} depends on the fact that we have used as input only the oscillator strength of the two-photon transition, which correspond to the square modulus of the effective matrix element; the phase difference between this matrix element and the one resulting from the one-photon transition is thus not determined. The proportionality of the coupling β to the square root of the generalized oscillator strength is analogous to the classical vacuum Rabi splitting, in which the Rabi frequency is proportional to the square root of the density of resonant atoms or quantum wells.[41]

After having determined the general expressions for the coupling constant β in both the SHG and TPA cases, it can be interesting to present a few examples of its evaluation in specific cases of experimental interest. For illustrative purposes, the configurations chosen are amenable to transparent analytical calculations. Better experimental arrangements would require a careful numerical optimization of the structures.

We shall at first concentrate our attention on the nonlinear Rabi frequency $\Omega=|\beta B_1|$ as function of the internal intensity on the fundamental mode in a SHG configuration. For a simple metallic planar cavity of length L and dielectric constant $\epsilon(\omega)$, the wave function of the photonic modes are given by the expression

$$\mathcal{E}_j=\sqrt{\frac{4\pi\hbar\omega_j}{L\epsilon(\omega_j)}}\sin[\sqrt{\epsilon(\omega_j)}\omega_j x/c]; \tag{5.9}$$

where the ω_j have to satisfy the resonance condition

$$\omega_j = \frac{\pi c j}{L\sqrt{\epsilon(\omega_j)}}. \tag{5.10}$$

As function of the field amplitude A_1, the internal light intensity in each propagation direction of the fundamental mode can thus be written as

$$I_{int} = \frac{c\sqrt{\epsilon}}{4\pi}|\mathcal{E}_1 b_1|^2 = \frac{\hbar\omega_1 c}{L\sqrt{\epsilon(\omega_1)}}|A_1|^2, \tag{5.11}$$

where $\mathcal{E}_1$ has been taken at an antinode of the cavity mode.

According to the considerations worked out by Berger,[14] second harmonic generation in a metallic mirror microcavity is most effective when the cavity length L is close to the second harmonic generation coherence length L_{coh} of the nonlinear material; for GaAs at the technologically useful wavelength of 10.6 μm the slight difference between $\epsilon(\omega_1)$ and $\epsilon(\omega_2)$ gives a coherence length equal to 108 μm. In this specific geometrical arrangement, explicit integration of Eq. (5.2) brings to the result:

$$\beta_{SHG} = 4\chi^{(2)}\sqrt{\frac{2\pi\hbar\omega_1}{L\epsilon^3}}\omega_1, \tag{5.12}$$

where we have set $\epsilon = \epsilon(\omega_1) \simeq \epsilon(\omega_2)$.

Using Eqs. (5.11) and (5.9), the nonlinear Rabi frequency $\Omega = |\beta A_1|$ can be written in terms of the internal light intensity I_{int} as

$$\frac{\Omega}{\omega_1} = 4\sqrt{\frac{2\pi I_{int}}{\epsilon^{5/2}c}}\chi^{(2)}. \tag{5.13}$$

The experimental value of $\chi^{(2)}$ for GaAs at 10.6 μm is about 2.4×10^{-7} esu.[16,42] So, in order to observe the splitting, assuming that the cavity quality factor is $Q=10^4$, it is necessary to have Ω/ω_1 at least equal to 10^{-4}; this is satisfied provided the internal power is about 1 GW cm^{-2}. As long as the nonlinear material fills the entire cavity, a change in the cavity length does not affect β; to increase β we thus have to increase $\chi^{(2)}$ shifting the operating frequency closer to the gap edge or changing the nonlinear medium.

The present calculation has considered metallic mirrors mainly because of analytical convenience, however it could be generalized to the case of a dielectric microcavity with DBR mirrors optimized for reflection at both the fundamental and at the harmonic frequency (FASH mirrors[14]). Such mirrors, giving much more freedom in the choice of the reflection phase should facilitate the achievement and the stability of the double resonance condition, but at the same time the optical modes would penetrate inside the mirrors and an active material concentrated in the cavity layer would not be the best alternative any more; in this case it may be better to distribute the nonlinearity along the whole effective length of the cavity mode. Although such an arrangement has revealed to be useful for optical bistability and optical ''transistor'' effect,[10,11] it has not been studied yet for optimizing second harmonic generation.

Two-photon absorption spectroscopy has been an important tool for the characterization of electron-hole states in quantum wells: the two-photon absorption spectra taken at $\omega \simeq E_G/2$ show in fact sharp features due to subband quantization and excitonic effects.[43–45] In particular it has been possible to clearly resolve some excitonic peaks. Provided their linewidth is sufficiently small, these transitions seems to be a good candidate for the observation of our coherent two-photon effects. Since the sharpest features are present in TM polarization ($\hat{\epsilon}\|\hat{z}$), it is necessary to work at oblique incidence. This is not a problem, indeed it gives the possibility of tuning the photonic fundamental mode with the angle, while the excitonic frequency stays nearly constant. A detailed calculation of the two-photon absorption cross-section in GaAs/$Al_xGa_{1-x}As$ heterostructures has been performed by Shimizu.[35] For example, conversion of his results for the c_1lh_2,1S exciton into generalized oscillator strengths brings to the result of about $f_{2D}^{(3)} \simeq 2\times10^{-29}$ cm^4. It can be interesting to notice that, if we assume a linewidth of 1 meV for the exciton and a well spacing of 10 nm, this value corresponds to a resonant $\chi^{(3)}$ of 1.2×10^{-8} esu. Moreover, under a strong static-electric field parallel to the growth axis, some excitonic transitions can be allowed for both one- and two-photon absorption because of parity symmetry breaking.[35] But an externally applied static-electric field is not the only solution: several papers have appeared which investigate the problem of breaking the symmetry of a material system in order to make some optical susceptibility nonvanishing. In particular, asymmetrically grown quantum wells[36,37] and indirect excitons in polytype double-quantum-well structures[38] have recently received much interest.

We consider a microcavity of effective mode length L_{eff} (Ref. 46) and dielectric constant ϵ bounded by dielectric mirrors containing N_w identical quantum wells situated at positions $x_{1\ldots N_w}$ all corresponding to antinodes of the electric field; in this case the generalized oscillator strength $f^{(3)}(x)$ is given by

$$f^{(3)}(x) = \sum_{i=1}^{N_w} f_{2D}^{(3)}\delta(x - x_i). \tag{5.14}$$

Explicit integration of Eq. (5.8) then brings to the result

$$\beta_{TPA} \simeq \frac{\pi\omega_1}{L_{eff}\epsilon}\sqrt{24 f_{2D}^{(3)} N_w}. \tag{5.15}$$

Using again Eqs. (5.11) and (5.9), the Rabi frequency can be written as function of internal light intensity I_{int} as

$$\frac{\Omega}{\omega_1} \simeq \sqrt{\frac{24 N_w f_{2D}^{(3)}\pi^2 I_{int}}{L_{eff}\epsilon^{3/2}\hbar\omega_1 c}}. \tag{5.16}$$

As previously, we can quantify the effect in terms of the internal intensity needed in order to have $\Omega/\omega_1 = Q^{-1} \simeq 10^{-3}$.[47] Inserting the numerical values for the quantum well excitonic transition and supposing $N_w/L_{eff} \simeq 5/\lambda$, we obtain an internal intensity of about 1.2 GW cm^{-2}.

While in the SHG case the main limitation on light intensity comes from unavoidable heating effects, in the TPA case it is necessary to pay attention also to the fact that excitons behave in a bosonic way only at low densities $n_{exc} \ll n_{sat}$,[34] i.e., when their mean spacing is much larger than their radius. At higher densities, in fact, both screening effects and the fermionic nature of the underlying electrons and holes

contribute to bleach the excitonic transition. Remembering that the total population of excitons per unit area is given by $|A_2|^2$ and assuming the excitons are equally distributed among the wells, it follows from Eq. (2.7) that the excitonic density in each well has the expression

$$n_{exc}=|A_2|^2/N_w=\left|\frac{\Omega^2}{2\omega_L-\omega_2+i\gamma_2}\right|^2\frac{1}{N_w|\beta|^2}; \quad (5.17)$$

inserting in this expression a realistic value for β in GaAs structures, it results that the two-photon Rabi splitting should be observable in GaAs structures before the exciton is bleached, while for the instabilities and the TPOSE gain the required excitonic density turns out much higher than the typical saturation density of about $n_{sat}=3\times10^{11}$ cm^{-2}. However, in order to obtain a given value of the nonlinear effects (i.e., the minimum observable one: $\Omega/\omega_1\simeq1/Q$) an increased nonlinear coupling β or a larger number of wells N_w could be employed giving rise to a lower excitonic density n_{exc}.

Finally, we remark that in all cases the relevant physics is determined by the internal intensity of the fundamental mode. For a given experimental arrangement, the corresponding pump incident intensity mainly depends on the reflectivity R of the mirrors [through the coefficients $\gamma_1\simeq c(1-R)/2L_{eff}$ and $k_1\simeq\sqrt{c\gamma_1/2}$ in Eqs. (2.1)–(2.3)] and on the detuning from the dressed modes of the cavity [see Eq. (2.6)] as can be observed in Fig. 1.

VI. CONCLUSIONS

We have studied nonlinear optical effects arising in a microcavity geometry from doubly-resonant second harmonic generation (SHG) and resonant two-photon absorption (TPA). In particular, we have discussed the effect of a nonlinear cubic coupling between two bosonic modes on both the transmission spectrum of the cavity and pump-and-probe experiments.

Recovering and completing some early results, we have found that the transmission spectrum of the cavity is characterized by a doublet of peaks the position and relative weight of which depends on light intensity; a physical interpretation of the results in terms of a simple two-level model with intensity-dependent coupling (two-photon Rabi splitting) has been put forward.

In analogy to classical papers on the optical Stark effect in driven two-level systems, we have studied how the optical response of our system to a weak probe beam is modified by the presence of a strong pump beam, giving rise to a two-photon optical Stark effect (TPOSE). For moderate pump intensities a simple two-level picture with intensity-dependent coupling can again account for the features resulting from the calculations. At higher pump intensities interesting new features are predicted: in particular, the analogue of stimulated hyper-Raman scattering can give rise even to some gain in well-determined spectral regions. Even in such a case, the nonlinear absorption sum rule is satisfied independently of pump intensity.

We have also investigated the feasibility of the proposed experiments in realistic GaAs-based systems: in both the SHG and the TPA cases, the required internal intensity results of the order of 1 GW cm^{-2}. While in the SHG case the most stringent limitation on light intensity comes from the optical damage threshold of the structure, in the TPA case it is also necessary to pay attention to the possibility of bleaching the excitonic oscillator strength at high-excitonic densities. In any case, the continuous improvement of sample quality is expected to enhance the sharpness of the spectral features, so that a better resolution of line-splittings and absorption-gain signals will allow for the observation of such nonlinear effects at lower light intensities and lower excitonic densities.

Even if the numerical estimates refer only to the case of GaAs-based microstructures, they illustrate how to evaluate the coupling coefficients appearing in our model Hamiltonian for a given experimental arrangement. Our theoretical approach is in fact completely general and can be applied to a variety of other interesting systems, e.g., organic microcavities;[48] the use of such materials can be convenient because of stronger second harmonic generation[49] and larger oscillator strength and saturation density of the excitonic resonance of molecular semiconductors.[50]

ACKNOWLEDGMENTS

It is a pleasure to thank L.C. Andreani, M. Artoni, F. Bassani, C. Ciuti, V. Lucarini, V. Pellegrini, and V. Savona for valuable discussions; one of us (I.C.) is especially grateful to M. Inguscio and F. Beltram for their continuous encouragement and interest. Partial financial support from the MURST grant ''Fisica delle nanostrutture'' is acknowledged.

[1] C. Cohen-Tannoudji, J. Dupont-Roc, and Gilbert Grynberg, *Processus d'Interaction Entre Photons et Atomes* (InterEditions/ Editions du CNRS, Paris, 1988).

[2] M.D. Levenson and S.S. Kano, *Introduction to Nonlinear Laser Spectroscopy* (Academic Press, New York, 1987).

[3] C.S. Adams and E. Riis, Prog. Quantum Electron. **21**, 1 (1997).

[4] See the articles in *Confined Electrons and Photons*, edited by C. Weisbuch and E. Burstein (Plenum Press, New York, 1995).

[5] H. Haug and S.W. Koch, *Quantum Theory of the Optical and Electronic Properties of Semiconductors* (World Scientific, Singapore, 1993).

[6] P.N. Butcher and D. Cotter, *The Elements of Nonlinear Optics* (Cambridge University Press, Cambridge, 1993).

[7] C. Weisbuch, M. Nishioka, A. Ishikawa, and Y. Arakawa, Phys. Rev. Lett. **69**, 3314 (1992); R. Houdré, R. P. Stanley, U. Oesterle, M. Ilegems, and C. Weisbuch, Phys. Rev. B **49**, 16 761 (1994).

[8] T.B. Norris, J. K. Rhee, D. S. Citrin, M. Nishioka, and Y. Ar-

akawa, Nuovo Cimento D **17**, 1295 (1995); A. Tredicucci, Y. Chen, V. Pellegrini, M. Börger, and F. Bassani, Phys. Rev. A **54**, 3493 (1996).
[9] S. Savasta, R. Girlanda, and G. Martino, Phys. Status Solidi **164**, 85 (1997).
[10] I. Carusotto and G.C. La Rocca, Phys. Lett. A **243**, 236 (1998).
[11] I. Carusotto and G.C. La Rocca, Phys. Status Solidi **164**, 377 (1997).
[12] F. Quochi, G. Bongiovanni, A. Mura, J. L. Staehli, B. Deveaud, R. P. Stanley, U. Oesterle, and R. Houdré, Phys. Rev. Lett. **80**, 4733 (1998).
[13] C. Ciuti and F. Quochi, Solid State Commun. **107**, 715 (1998).
[14] V. Berger, J. Opt. Soc. Am. B **14**, 1351 (1997).
[15] C. Zimmermann, R. Kallenbach, T.W. Hänsch, and J. Sandberg, Opt. Commun. **71**, 229 (1989); C. Simonneau, J. P. Debray, J. C. Harmand, P. Vidaković, D. J. Lovering, and J. A. Levenson, Opt. Lett. **22**, 1775 (1997).
[16] E. Rosencher, B. Vinter, and V. Berger, J. Appl. Phys. **78**, 6042 (1995).
[17] R. Paschotta, K. Fiedler, P. Kürz, and J. Mlynek, Appl. Phys. B: Lasers Opt. **58**, 117 (1994).
[18] S. Haroche and F. Hartmann, Phys. Rev. A **6**, 1280 (1972).
[19] B.R. Mollow, Phys. Rev. A **5**, 2217 (1972).
[20] F.Y. Wu, S. Ezekiel, M. Ducloy, and B.R. Mollow, Phys. Rev. Lett. **38**, 1077 (1977).
[21] K.J. McNeil, P.D. Drummond, and D.F. Walls, Opt. Commun. **27**, 292 (1978).
[22] P.D. Drummond, K.J. McNeil, and D.F. Walls, Opt. Commun. **28**, 255 (1979).
[23] P.D. Drummond, K.J. McNeil, and D.F. Walls, Opt. Acta **27**, 321 (1980).
[24] P.D. Drummond, K.J. McNeil, and D.F. Walls, Opt. Acta **28**, 211 (1981).
[25] P. Mandel, N.P. Pettiaux, W. Kaige, P. Galatola, and L.A. Lugiato, Phys. Rev. A **43**, 424 (1991).
[26] S.E. Harris, Phys. Rev. Lett. **62**, 1033 (1989).
[27] D.F. Walls, P.D. Drummond, and K.J. McNeil, in *Optical Bistability*, edited by C.M. Bowden, M. Ciftan, and H.R. Robl (Plenum Press, New York, 1981).
[28] M.J. Collett and D.F. Walls, Phys. Rev. A **32**, 2887 (1985).
[29] G.S. Agarwal, Phys. Rev. Lett. **73**, 522 (1994).
[30] L.D. Landau and E.M. Lifshitz, *Mechanics* (Pergamon Press, Oxford, 1960).
[31] H.J. Kreuzer, *Nonequilibrium Thermodynamics and its Statistical Foundations* (Clarendon Press, Oxford, 1981).
[32] B.R. Mollow, Phys. Rev. **188**, 1969 (1969).
[33] F.Y. Wu, R.E. Grove, and S. Ezekiel, Phys. Rev. Lett. **35**, 1426 (1975).
[34] S. Schmitt-Rink, D.S. Chemla, and D.A.B. Miller, Phys. Rev. B **32**, 6601 (1995).
[35] A. Shimizu, Phys. Rev. B **40**, 1403 (1989).
[36] E. Rosencher and Ph. Bois, Phys. Rev. B **44**, 11 315 (1991).
[37] V. Pellegrini, A. Parlangeli, M. Börger, R. D. Atanasov, and F. Beltram, Phys. Rev. B **52**, R5527 (1995).
[38] C. Ciuti and G.C. La Rocca, Phys. Rev. B **58**, 4599 (1998).
[39] J.P. Likforman, M. Joffre, and D. Hulin, Phys. Rev. Lett. **79**, 3716 (1997).
[40] F. Bassani and S. Scandolo, Phys. Rev. B **44**, 8446 (1991); S. Scandolo and F. Bassani, *ibid.* **45**, 13 257 (1992).
[41] G.S. Agarwal, Phys. Rev. Lett. **53**, 1732 (1984).
[42] S. Scandolo and F. Bassani, Phys. Rev. B **51**, 6928 (1994).
[43] K. Tai, A. Mysyrowicz, R.J. Fischer, R.E. Slusher, and A.Y. Cho, Phys. Rev. Lett. **62**, 1784 (1989).
[44] A. Pasquarello and A. Quattropani, Phys. Rev. B **38**, 6206 (1988).
[45] I.M. Catalano, A. Cingolani, R. Cingolani, M. Lepore, and K. Ploog, Phys. Rev. B **40**, 1312 (1989); I.M. Catalano, A. Cingolani, R. Cingolani, M. Lepore, and K. Ploog, Solid State Commun. **71**, 217 (1989).
[46] G. Panzarini, L. C. Andreani, A. Armitage, D. Baxter, M. S. Skolnick, V. N. Astratov, J. S. Roberts, A. V. Kavokin, M. R. Vladimirova, and M. A. Kaliteevski, Phys. Rev. B **59**, 5082 (1999).
[47] A. Fainstein and B. Jusserand, Phys. Rev. B **57**, 2402 (1998).
[48] D.G. Lidzey, T. Virgili, D. D. C. Bradley, M. S. Skolnick, S. Walker, and D. M. Whittaker, Nature (London) **395**, 53 (1998); T. Fujita, Y. Sato, T. Kuitani, and T. Ishihara, Phys. Rev. B **57**, 12 428 (1998).
[49] C. Bosshard, K. Sutter, Ph. Prêtre, J. Hulliger, M. Flörsheimer, P. Kaatz, and P. Günter, *Organic Nonlinear Materials* (Gordon and Breach, Basel, 1995).
[50] V.M. Agranovich, D.M. Basko, G.C. La Rocca, and F. Bassani, J. Phys.: Condens. Matter **10**, 9369 (1998).